



ELSEVIER

15 January 1999

OPTICS
COMMUNICATIONS

Optics Communications 159 (1999) 237–242

Ultrashort pulse generation in cw solid-state lasers with semiconductor saturable absorber in the presence of the absorption linewidth enhancement

V.L. Kalashnikov, D.O. Krimer, I.G. Poloyko^{*}, V.P. Mikhailov*International Laser Center, 65 Skorina Avenue, Building 17, Minsk 220027, Belarus*

Received 23 July 1998; revised 7 October 1998; accepted 4 November 1998

Abstract

A theory for ultrashort pulse generation in cw solid-state lasers with a 'slow' semiconductor saturable absorber in the presence of self-phase modulation in the active medium and absorption linewidth enhancement in the semiconductor has been developed. It was shown that with increase of pump energy the laser switches from stable ultrashort pulse generation to bistable operation regime. The parameters for stable ultrashort pulse generation were found. © 1999 Elsevier Science B.V. All rights reserved.

Keywords: Ultrashort pulse generation; Solid-state laser; Semiconductor saturable absorber

1. Introduction

Over the past few years a considerable progress has been made in femtosecond solid-state lasers. It was connected mainly to exploitation of the fast electronic nonlinearity, which causes Kerr lensing [1] and has a response time of the order of few femtoseconds. On the other hand, an efficient mode-locking in the femtosecond time domain has been achieved with semiconductor saturable absorbers [2–4]. The fastest excitation decay time T_a of the semiconductor absorbers used in the experiments was approximately 100 fs, which according to the ordinary theory of passive mode-locking prevents ultrashort pulse generation with duration of tens of femtoseconds. To explain the extremely short pulse generation, a soliton mode-locking mechanism has been proposed [5]. This mechanism involves the combined action of the group velocity dispersion (GVD) and the fast nonlinear refraction producing

self-phase modulation (SPM). Kärtner et al. [5] noted also that the 'slow' nonlinear refraction in the semiconductor absorber (so-called linewidth enhancement) can stabilize an ultrashort pulse.

It is known that the semiconductor structures used as passive modulators possess an extremely high nonlinearity, which depends on the carrier density and, consequently, on the pulse energy (see, for example, Ref. [6]). This produces a strong energy-dependent SPM, which is proportional to the loss coefficient. The corresponding coefficient of proportionality (Henry's factor) is about -3 to -8 [7,8].

Here we present a theory for ultrashort pulse generation in cw solid-state lasers in the presence of fast nonlinear refraction in the active medium and carrier density-dependent SPM in the semiconductor absorber. As we shall demonstrate later on, the last factor essentially transforms the pulse characteristics and can stabilize an ultrashort pulse against automodulational instability. Also absorber linewidth enhancement produces negative feedback, that leads to multistable operation. One should note the difference from an existing theory [5], where quasi-Schrödinger laser solitons were studied.

^{*} Corresponding author. E-mail: ilc@user.unibel.by

2. Discussion

Based on the self-consistent field theory [9] and taking into account the gain, saturable loss in the semiconductor, frequency filtering, GVD and SPM, we arrive at the master equation:

$$\begin{aligned} \frac{\partial a(k,t)}{\partial k} = & \left\{ \alpha - \Gamma \exp\left(-\frac{1+i\chi}{U_a} \varepsilon\right) \left(1 + \frac{\partial}{\partial t}\right)^{-1} \right. \\ & + \left[\left(1 + \frac{\partial}{\partial t}\right)^{-1} - 1 \right] - l + id \frac{\partial^2}{\partial t^2} - i\beta |a|^2 \\ & \left. + i\phi \right\} a(k,t), \end{aligned} \quad (1)$$

where $a(k,t)$ is the field, k is the transit number, t is the local time, α is the dynamically saturated gain, Γ is the initial loss of the absorber, χ is the Henry factor, U_a is the saturation energy of the absorber, $\varepsilon = \int_{t_0}^t |a(k,t')|^2 dt'$ is the pulse energy (t_0 is the time moment corresponding to the pulse peak), l is the linear loss, d is the GVD coefficient, β is the SPM coefficient of the active medium, ϕ is the phase delay after the full round trip. The term in square brackets describes the frequency filter. Operator $(1 + \partial/\partial t)^{-1}$ is effective only with respect to the field a , not to the energy ε . In Eq. (1) all times are normalized by the inverse filter bandwidth t_f . For simplicity, we assume an equal bandwidth for the loss and frequency filter and neglect the gain dispersion.

An expansion of Eq. (1) into a series in energy ε accounting for the dynamical loss and gain saturation by pulse energy yields:

$$\begin{aligned} \frac{\partial a(k,t)}{\partial k} = & \left\{ \alpha_0 \left(1 - \tau\varepsilon + \frac{(\tau\varepsilon)^2}{2}\right) - l - \gamma_0 \right. \\ & - \gamma_0(1+i\chi) \left(\frac{\varepsilon^2}{2} - \varepsilon\right) \\ & - (1 - \gamma_0(1 - \varepsilon)) \frac{\partial}{\partial t} \\ & + (1 - \gamma_0) \frac{\partial^2}{\partial t^2} + id \frac{\partial^2}{\partial t^2} \\ & \left. - i\chi\gamma_0\varepsilon \frac{\partial}{\partial t} + i\phi - ip|a(k,t)|^2 \right\} a(k,t), \end{aligned} \quad (2)$$

where α_0 and γ_0 are the saturated gain and the saturated loss at the pulse peak, respectively. In Eq. (2) the pulse energy is normalized by the saturation energy of the absorber U_a , τ is the ratio of the loss saturation energy to the gain saturation energy (taking into account the mode cross-sections at the absorber and at the active medium), $p = \beta U_a/t_f$. In order to derive an exact steady-state solution of Eq. (2), we neglected the higher-order terms $(\varepsilon^2/2)\gamma_0^0(\partial/\partial t)$, $\gamma_0(\varepsilon - \varepsilon^2/2)(\partial^2/\partial t^2)$, $i\chi\gamma_0\varepsilon(\partial^2/\partial t^2)$, $i\chi\gamma_0\varepsilon^2(\partial/\partial t - \partial^2/\partial t^2)/2$. The correctness of this approximation was checked by applying a perturbation theory analysis.

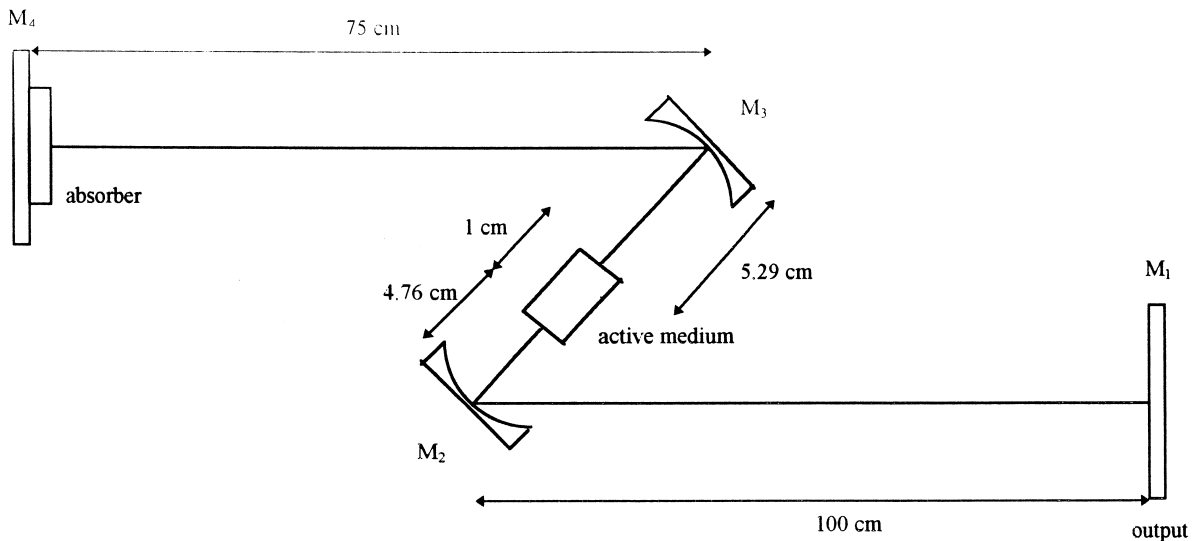


Fig. 1. The resonators configuration for passive mode-locking with semiconductor absorber. $M_{1,2,3,4}$ are the mirrors, the curvature radius of the folding mirrors is 10 cm.

The soliton-like solution of Eq. (2) is

$$a(k, t) = a_0 \operatorname{sech}^{1+i\psi} \left[(t - k\delta) / t_p \right] \exp[i\omega t], \quad (3)$$

where a_0 is the pulse amplitude, δ is the round-trip delay so that $t_0 = k\delta$, t_p is the pulse duration, ω is the frequency shift from the gain center. Substitution of the expression (3) into (2) gives a set of six algebraic equations. As the solution is quite clumsy, we write here only the expression for the pulse duration:

$$t_p = \sqrt{\frac{1 - \gamma_0 - d\psi}{\alpha_0 - \gamma_0 - \omega^2 + \gamma_0 \omega^2}}.$$

To relate the parameters of our model to those available in the experiment, we have to recalculate the saturated loss at pulse peak γ_0 with respect to the initial saturable loss Γ : $\gamma_0 = \Gamma e^{-E/2}$ assuming that the loss recovery time is much shorter than the cavity period T_{cav} and much longer than the pulse duration. Here $E = \int_{-\infty}^{\infty} |a|^2 dt$ is the full pulse energy. Although in typical femtosecond lasers, the gain saturation energy is much larger than the loss saturation energy (in our calculations $\tau = 0.0015$, which corresponds to the loss saturation fluence of $100 \mu\text{J}/\text{cm}^2$ and Ti:sapphire active medium with the beam radius at the active medium of $30 \mu\text{m}$, and at the absorber of $106 \mu\text{m}$, see Fig. 1), our calculations have shown that the balance between these two factors noticeably affects ultrashort pulse parameters. Accounting for the gain saturation is performed as follows:

$$\alpha_0 = \alpha_m \frac{1 - \exp(-U)}{1 - \exp(-U - \tau E)} \exp(-\tau E/2),$$

where U is the pump intensity normalized by $\sigma_{14} T_{\text{cav}} / h\nu$, $h\nu$ is the pump photon energy, σ_{14} is the absorption cross-section of the active medium, α_m is the gain at full

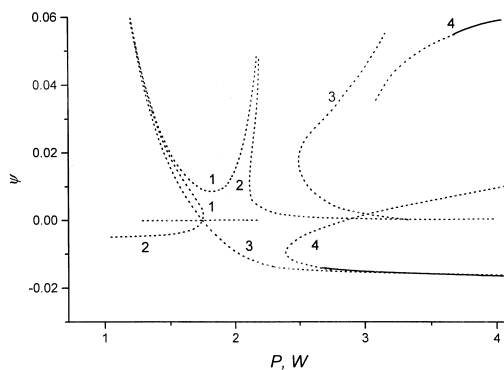


Fig. 2. Pulse chirp χ versus pump power P for different linewidth enhancement factors: $\chi = 0$ (1), -0.005 (2), -0.05 (3), -2.5 (4). Every parameter set has two solutions. Stable solutions are plotted by solid lines. GVD coefficient is -360 fs^2 , $\Gamma = 0.05$, $l = 0.05$, $\alpha_m = 1.5$, $p = 3$.

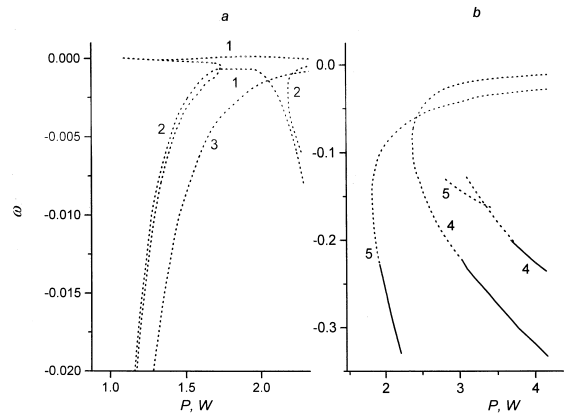


Fig. 3. Pulse frequency shift ω versus pump power P for different linewidth enhancement factors and GVD coefficients: $\chi = 0$ (1), -0.005 (2), -0.05 (3), -2.5 (4,5); $d = -360 \text{ fs}^2$ (1–4), -90 fs^2 (5). Other parameters are as in Fig. 2. Stable solutions are plotted by solid lines. To better illustrate the behavior of the curves the plot is divided into parts (a) and (b).

inversion, T is the gain recovery time normalized by T_{cav} . This equation gives an additional condition for determining the pulse parameters.

As our analysis showed, in the absence of SPM ($p = 0$ in Eq. (2)) there is strong domination of slow loss saturation over gain saturation, which is the case for solid-state lasers, the range of pump powers that provides femtosecond pulse generation is very small and, as was shown in Ref. [5], the pulse is unstable against laser noise.

The presence of SPM in the active medium ($p \neq 0$ in Eq. (2)) transforms the situation essentially. There appear two different solutions (Fig. 2, curves 1, where the solid lines denote a stable solution). The difference in the nature of these two solutions is explained by contribution from different pulse-forming mechanisms: (1) Schrödinger soli-

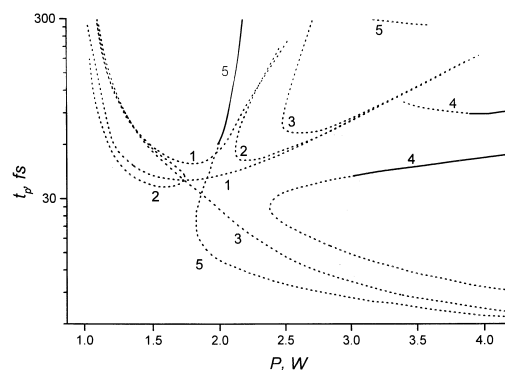


Fig. 4. Pulse duration t_p versus pump power P for different linewidth enhancement factors and GVD coefficients: $\chi = 0$ (1), -0.005 (2), -0.05 (3), -2.5 (4,5); $d = -360 \text{ fs}^2$ (1–4), -90 fs^2 (5). Other parameters are as in Fig. 2. Stable solutions are plotted by solid lines.

ton mechanism, producing a chirp-free pulse with zero frequency shift and (2) ‘laser’ (dissipative) mechanism, producing essentially a chirped quasi-soliton with nonzero frequency shift (curves 1, Fig. 3a). Both solutions have a minimum in duration for certain pump power and GVD (Fig. 4, curves 1) and nearly linear dependence of the energy on the pump power (Fig. 5, curves 1).

Even a small energy-dependent nonlinear refraction ($\chi \neq 0$ in Eq. (2)) ‘mixes’ these two states, so that chirp compensation is possible only for relatively large pump (Fig. 2, curves 2, 3) and for the shortest pulse the chirp remains uncompensated (Fig. 4, curves 2, 3). The main features in the pulse parameters’ behavior in the presence of linewidth enhancement are broadening of the pump power region where ultrashort pulse generation is possible (the growth of the maximal pump power) and increase of the Stokes shift of the pulse carrier frequency. The latter factor produces a negative feedback due to the shift of the pulse spectrum from the gain band that decreases the pulse energy for large pump powers (Fig. 5, curve 3) and broadens the region of pulse existence.

Further increase of $|\chi|$ up to the magnitude typical for semiconductor absorbers increases the Stokes shift of the pulse (Fig. 3b, curves 4), so that a transform limited pulse exists for fixed GVD, only for some definite pump power (Fig. 2, curves 4). Strong negative feedback due to the frequency shift produces a negative slope in the dependence of the pulse energy on pump power (Fig. 5, curves 3–5). With decrease of $|d|$, the difference between pulse durations corresponding to the different branches of the solutions increases (Fig. 4, curves 5). The stable branch demonstrates dramatic growth (up to picosecond level) of the pulse duration under small pump power variation.

The regions of pulse existence are shown in Fig. 6. It is seen (Fig. 6a) that for fixed pump an optimal χ exists, which provides the broadest one in terms of GVD region of pulse existence. The regions of pulse existence are very

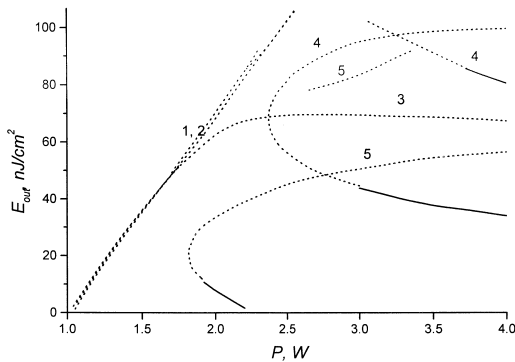


Fig. 5. Pulse energy fluence E_{out} versus pump power P for different linewidth enhancement factors and GVD coefficients: $\chi = 0$ (1), -0.005 (2), -0.05 (3), -2.5 (4, 5); $d = -360 \text{ fs}^2$ (1–4), -90 fs^2 (5). Other parameters are as in Fig. 2. Stable solutions are plotted by solid lines.

sensitive to the pump power (Fig. 6b). The lowest threshold of pump powers necessary for ultrashort pulse generation is provided by some small negative GVD ($\approx -200 \text{ fs}^2$), where negative feedback is minimal and the pulse formation is due to the soliton mode-locking mechanism. However, as we shall demonstrate later on, this regime is not optimal for pulse stabilization.

Now we have to investigate the stability of the quasi-soliton. The stability against small perturbations of the pulse parameters (i.e., amplitude, duration, frequency shift, chirp and energy) is considered. Substituting the perturbed solution (3) into Eq. (2) and expanding it into a series in time, we obtain a set of equations set for the evolution of the pulse parameters:

$$\frac{da_0}{dk} = a_0 \left[\alpha_0 - \gamma_0 - l - \omega^2(1 - \gamma_0) - v(1 - \gamma_0 - d\psi) \right], \quad (4a)$$

$$\frac{d\omega}{dk} = a_0^2 \left[\gamma_0(\chi - \omega - \psi - \chi\omega\psi) + \alpha_0 a_0^2 \psi \tau + 2v\omega(\gamma\psi^2 + \gamma_0 - \psi^2 - 1) \right], \quad (4b)$$

$$\frac{dv}{dk} = a_0^4 (\gamma_0 - \alpha_0 \tau^2) + 2a_0^2 \gamma_0 v (\chi\psi - 1) + 2v^2 (3d\psi + \psi^2 + \gamma_0 - \gamma_0\psi - 1), \quad (4c)$$

$$\frac{d\psi}{dk} = -2a_0^2 (\gamma_0 \chi + p + \gamma_0 \chi \psi^2) + \frac{a_0^4}{v} (\gamma_0 \chi - \gamma_0 \psi + \alpha_0 \tau^2 \chi) + 2v (\gamma_0 \psi^2 + \psi \gamma_0 - 2d\psi^2 - \psi^2 - 2d), \quad (4d)$$

where $v = 1/t_p^2$.

Stability analysis for the energy perturbation follows the scheme presented in Ref. [10]: integration of Eq. (2) and summing up with its complex conjugate gives the pulse energy conservation law. From this integral of motion, the condition for the decay of the perturbation of the pulse energy follows:

$$-\alpha_0 \tau e^{\tau E/2} (1 + e^{-\tau E}) + l + \Gamma(1 + e^{-E}) - \frac{2\sqrt{v}}{3} (1 - \gamma_0) (1 + \psi^2 + 3\omega^2/v) - \frac{2}{3} \gamma_0 a_0^2 (\chi\psi - 1) < 0. \quad (5)$$

Here we assumed that the loss and gain saturation obey an exponential law, which is the case for a quasi-two-level system with a relaxation time much longer than the pulse duration.

The Jacobian of the set of Eqs. (4a), (4b), (4c), (4d) and (5) determines the condition for pulse stability against automodulational instabilities. It is seen from Eqs. (4a) and (5), that the frequency shift, chirp and spectral filtering

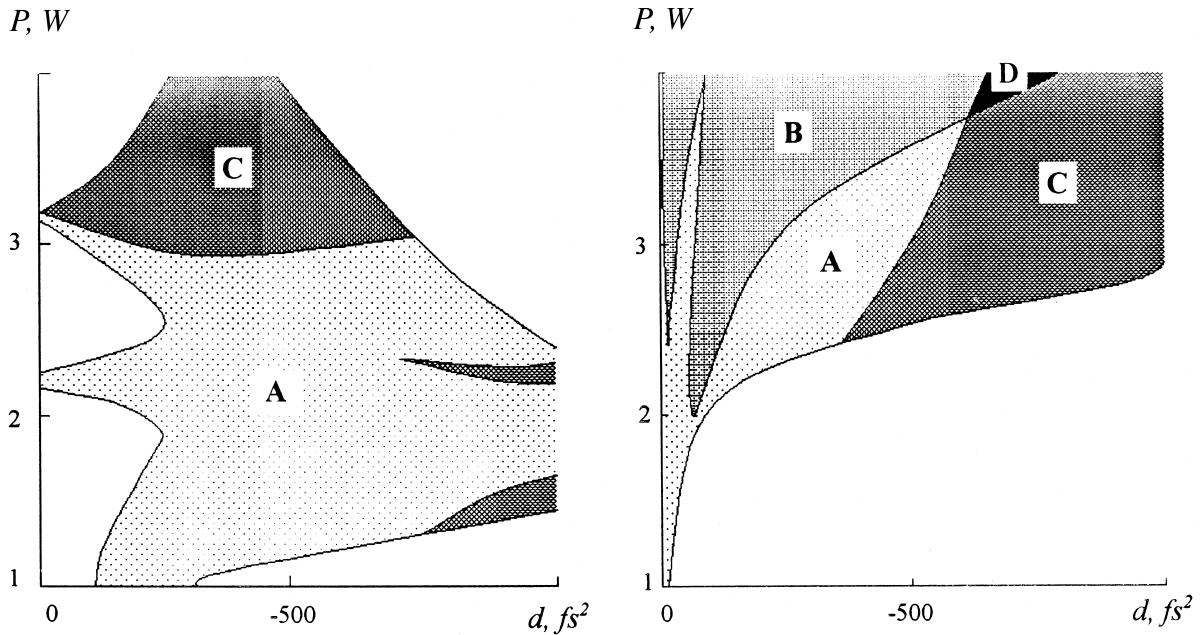


Fig. 6. Regions of pulse existence. (A) Region of instability, (B) automodulational stability, (C) stability against noise, (D) automodulational and noise stability on the plane (GVD–pump). $\chi = 0$ (a), -2.5 (b).

(fourth term in Eq. (5)) stabilize the pulse against energy and amplitude perturbations, ‘slow’ (first term in Eq. (4b) and second term in Eq. (4d)) and ‘fast’ (first term in Eq. (4d)) SPM stabilize the pulse against frequency and chirp perturbations. This stabilization is provided by negative feedback due to pulse chirping and frequency shift in the presence of finite gain and filter bandwidth.

Besides automodulational instabilities, there is another source of pulse destabilization, namely, laser continuum (noise). As was shown in Ref. [11], the main mechanism of laser noise suppression in this case is the difference in group velocities for the pulse and noise which produces a permanent walk-off of the noise out of the window of positive net-gain while the pulse matches it perfectly. Evolution of cw-noise N obeys the following equation:

$$\frac{dN(k,t)}{dk} = \left\{ \alpha_0 e^{-\tau E/2} - l - V - \delta \frac{\partial V}{\partial t} \right\} N(k,t), \quad (6)$$

where $V = \Gamma(1 + (e^{-E} - 1)e^{-t/T_a})$ is the ‘potential’ created by the pulse, the derivative describes the time shift of the noise with respect to the pulse. From Eq. (6) the condition for the noise energy decay follows:

$$\alpha_0 e^{-\tau E/2} - l - \Gamma e^{-E} - \frac{\delta}{T_a} \Gamma(1 - e^{-E}) < 0. \quad (7)$$

The solutions of Eq. (2) which are stable against automodulational instabilities are shown in Figs. 2–5 by solid lines. It should be noted that the soliton mode-locking mechanism does not work over the full region of pulse

existence which is evidenced by essentially nonzero chirp of the pulse. As it is seen from Figs. 2–5, a relatively large nonlinear refraction in the semiconductor causes bistable operation: there are two stable solutions (curves 4) that exist simultaneously around pump power of 4 W. One of these solutions has a smaller chirp (Fig. 2), larger Stokes shift (Fig. 3b), shorter duration (Fig. 4) and lower energy (Fig. 5).

Negative feedback due to absorption linewidth enhancement stabilizes the pulse against pulse energy perturbation. This is explained by the dependence of the pulse frequency shift on the pulse energy: the increase of the pulse energy produces a bigger frequency shift, which makes the pulse amplification inefficient due to the bad overlap of the pulse and gain spectrum. This prevents further growth of the pulse energy; the opposite situation prevents the decrease of the pulse energy. Thus, a negative slope efficiency of the stable solution (curves 4 in Fig. 5) has physical meaning.

Fig. 6 presents the regions of pulse existence. In area A the pulse is unstable. In area B the pulse is stable against automodulational instabilities, in area C the pulse is stable against laser continuum and in area D the pulse is stable against both automodulational and cw instabilities. It is seen that in the absence of linewidth enhancement the pulse is unstable against automodulational perturbations due to the absence of negative feedback (Fig. 6a). The increase of the negative linewidth enhancement factor increases the threshold of the pulse generation due to nonlinear loss produced by pulse frequency shift, but there

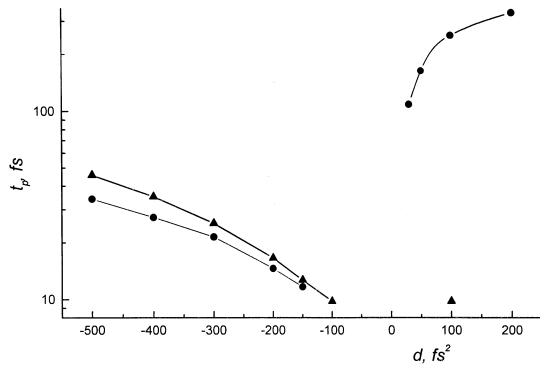


Fig. 7. Pulse duration t_p versus GVD d in the presence (triangles) and in the absence (circles) of slow SPM. (Numerical modeling.)

appears a region of automodulational stability which arises due to the ‘slow’ SPM in the semiconductor (Fig. 6b). This is accompanied by pulse shortening down to the shortest possible duration t_f and the region where the pulse is stable against both types of instabilities (area D in Fig. 6b).

For the most interesting region of the system’s parameters, where relatively small negative GVD provides pulse durations close to the shortest possible, we performed a numerical simulation. A three-level scheme was used for modeling the amplitude of the semiconductor absorber with 100 fs fast relaxation component and 1 ps slow relaxation component. The saturation energy fluence was taken to be 2 mJ/cm², other parameters were $p = 6$, $t_f = 3$ fs, $\Gamma = 0.05$, $U = 0.004$. In order to guarantee a good convergence of numerical procedure, we have chosen $\chi = -0.1$. However, even such small χ can stabilize an ultrashort pulse in the region of small $|d|$ (Fig. 7). Pulse duration versus GVD without (circles) and with (triangles) linewidth enhancement in the semiconductor is presented in Fig. 7. As is seen, a nonzero χ shifts the region of pulse existence into the positive direction of GVD (by approximately 100 fs²) in comparison to the situation with $\chi = 0$, the pulse duration being reduced from ≈ 13 to 9 fs. A distinctive feature of the contribution of slow nonlinear refraction is the generation of stable and extremely short pulses in the region of small positive GVD.

3. Conclusion

We have demonstrated the influence of absorption linewidth enhancement in a semiconductor on the ultrashort pulse characteristics in solid-state lasers. The linewidth enhancement introduces a negative feedback that stabilizes the pulse. The region of pulse stability is much wider in this case than in the case of the soliton stabilization mechanism. At low pump powers and low negative GVD a dramatic growth of the pulse duration is observed. Bistable operation for large pump powers is possible, too. Numerical simulation showed pulse shortening due to linewidth enhancement compared with usual soliton mode-locking for small negative GVD. The advantage of the mode-locking mechanism described above is the operation without Kerr-lensing, which is very attractive for diode-pumped cavity alignment in sensitive systems with large mode cross-section.

References

- [1] D.E. Spence, P.N. Kean, W. Sibbett, *Opt. Lett.* 16 (1991) 42.
- [2] U. Keller, K.J. Weingarten, F.X. Kärtner, D. Kopf, B. Braun, I.D. Jung, R. Fluck, C. Honninger, N. Matuschek, A. der Au, *IEEE J. Selected Topics Quantum Electron.* 2 (1996) 435.
- [3] P.T. Guerreiro, S. Ten, N.F. Borrelli, J. Butty, G.E. Jabbour, N. Peyghambarian, *Appl. Phys. Lett.* 71 (1997) 1595.
- [4] S. Tsuda, W.H. Knox, S.T. Cundiff, W.Y. Jan, J.E. Cunningham, *IEEE J. Selected Topics Quantum Electron.* 2 (1996) 454.
- [5] F.X. Kärtner, I.D. Jung, U. Keller, *IEEE J. Selected Topics Quantum Electron.* 2 (1996) 540.
- [6] H. Haug, S.W. Koch, *Quantum Theory of the Optical and Electronic Properties of Semiconductors*, World Scientific, 1994.
- [7] C.H. Henry, *IEEE J. Quantum Electron.* QE-18 (1982) 259.
- [8] M. Osinski, J. Buus, *IEEE J. Quantum Electron.* QE-23 (1987) 9.
- [9] H.A. Haus, *IEEE J. Quantum Electron.* QE-11 (1975) 736.
- [10] Sh. Namiki, E.P. Ippen, H. Haus, C.X. Yu, *J. Opt. Soc. Am. B* 14 (1997) 2099.
- [11] J.P. Gordon, *J. Opt. Soc. Am. B* 9 (1992) 91.